Journal for
ImmunoTherapy of Cancer

Quantitative tissue analysis and role of myeloid cells in non-small cell lung cancer

Brian S Henick [ID],[1] Franz Villarroel-Espindola [ID],[2] Ila Datar,[2] Miguel F Sanmamed,[3] Jovian Yu [ID],[4] Shruti Desai [ID],[3] Alice Li,[2,4] Adam Aguirre-Ducler,[2] Konstantinos Syrigos,[5] David L Rimm [ID],[2,3] Lieping Chen,[3] Roy S Herbst,[3] Kurt A Schalper [ID] [2,4]

[1]Medicine, Columbia University Irving Medical Center, New York, New York, USA
[2]Department of Pathology, Yale School of Medicine, New Haven, Connecticut, USA
[3]Yale Cancer Center, New Haven, Connecticut, USA
[4]Department of Medicine, Yale School of Medicine, New Haven, Connecticut, USA
[5]Sotiria General Hospital, National and Kapodistrian University of Athens, Athens, Athens, Greece

Correspondence to
Dr Kurt A Schalper;
kurt.schalper@yale.edu

ABSTRACT

Background Despite the prominent role of innate immunity in the antitumor response, little is known about the myeloid composition of human non-small cell lung cancer (NSCLC) with respect to histology and molecular subtype. We used multiplexed quantitative immunofluorescence (QIF) to measure the distribution and clinical significance of major myeloid cell subsets in large retrospective NSCLC collections.

Methods We established a QIF panel to map major myeloid cell subsets in fixed human NSCLC including 4',6-Diamidino-2-Phenylindole for all cells, pancytokeratin for tumor-epithelial cells, CD68 for M1-like macrophages; and CD11b plus HLA-DR to interrogate mature and immature myeloid cell populations such as myeloid derived suppressor cells (MDSCs). We interrogated 793 NSCLCs represented in four tissue microarray-based cohorts: #1 (Yale, n=379) and #2 (Greece, n=230) with diverse NSCLC subtypes; #3 (Yale, n=138) with molecularly annotated lung adenocarcinomas (ADC); and #4 (Yale, n=46) with patient-matched NSCLC and morphologically-normal lung tissue. We examined associations between marker levels, myeloid cell profiles, clinicopathologic/molecular variables and survival.

Results The levels of CD68+ M1 like macrophages were significantly lower and the fraction of CD11b+/HLA-DR− MDSC-like cells was prominently higher in tumor than in matched non-tumor lung tissues. HLA-DR was consistently higher in myeloid cells from tumors with elevated CD68 expression. Stromal CD11b was significantly higher in squamous cell carcinomas (SCC) than in ADC across the cohorts and EGFR-mutated lung ADCs displayed lower CD11b levels than KRAS-mutant tumors. Increased stromal CD68- and HLA-DR-expressing cells was associated with better survival in ADCs from two independent NSCLC cohorts. In SCC, increased stromal CD11b or HLA-DR expression was associated with a trend towards shorter 5-year survival.

Conclusions NSCLCs display an unfavorable myeloid immune contexture relative to non-tumor lung and exhibit distinct myeloid-cell profiles across histologies and presence of major oncogenic driver-mutations. Elevated M1-like stromal proinflammatory myeloid cells are prognostic in lung ADC, but not in SCC.

INTRODUCTION

Myeloid cells account for a large proportion of immune cells in blood and peripheral tissues, and they mediate innate inflammatory responses to eliminate foreign and potentially harmful agents. The landscape of myeloid cells is diverse and includes numerous cell subsets with distinct features and functional properties such as macrophages, antigen-presenting cells (APCs), granulocytes and natural killer cells.[1] In addition to their involvement in non-specific (eg, non-antigen-driven) innate immune responses, specialized myeloid cells such as macrophages and APCs can engage adaptive T-cell responses through phagocytosis, antigen presentation, and co-stimulation. Specialized myeloid cells with anti-inflammatory properties collectively termed myeloid-derived suppressor cells (MDSCs) can also exert prominent regulatory functions to limit inflammation and maintain tissue homeostasis.[1–4] The therapeutic value of manipulating myeloid cells to enhance antitumor immune responses is an area of active pre-clinical and clinical research. The possible role of tumor-associated myeloid cells in mediating sensitivity and resistance to T-cell-based immunostimulatory therapies remains poorly understood, though recently our group has demonstrated that CD68+ cells are the predominant immune cell type in non-small cell lung cancer (NSCLC) expressing programmed death ligand 1 (PD-L1), and that specifically increased PD-L1 levels in CD68+ macrophages predicts for improved overall survival in patients treated with programmed cell death protein-1 axis inhibitors.[5]

In addition to marrow-derived circulating myeloid cells such as granulocytes and monocytes, tissues contain resident macrophages whose differentiation is controlled

by complex transcriptional/epigenetic and microenvironmental programs.[2] [3] These cells are numerous, highly dynamic, and participate in specific tissue surveillance and particle/cell clearance functions. In the unaltered lung parenchyma, alveolar macrophages make up the largest proportion of cells in the alveolar space accounting for ~90% of the total cell population.[6] Additional macrophages can be found within the alveolar walls and peribronchial stromal tissue.

The microenvironment of NSCLC also contains large amounts of macrophages, termed tumor-associated macrophages (TAMs). The ontogeny of these cells is context-specific and may include both influx of blood monocytes and proliferation/differentiation of tissue-resident cells.[7] Most studies in human tumors and animal models support the notion that TAMs are not able to stimulate an effective inflammatory response and elevated macrophage densities are associated with adverse prognosis in multiple tumor types.[8–10] Similar to macrophages in non-tumor tissue, TAMs may have dissimilar and even opposite effects due to different functional programs. Although the functional profile of TAMs represents a delicate/stepwise process along a biological continuum,

two major macrophage polarization programs have been recognized and likely represent the extremes of this spectrum. These include classically polarized or M1-like TAMs with proinflammatory antitumor properties, and alternatively polarized or M2-like TAMs with regulatory function and associated with carcinogenesis and tumor progression.[10] A variety of markers including CD68, CD163, CD204, and HLA-DR have been used to identify TAM subtypes using immunohistochemistry in human malignancies, including lung cancer.[11] [12] However, results have been inconsistent with prominent technical limitations, such as the use of single markers and semi-quantitative analysis. Efforts have been recently undertaken to standardize the nomenclature of myeloid cell subpopulations to harmonize studies and data interpretation.[13] [14] Despite not capturing the complexity of all tumor-associated myeloid cells, it is generally accepted that co-expression of CD68 and the MHC-class II protein HLA-DR or CD80 can identify antitumor TAMs with M1-like phenotype, and positivity for myeloid markers such as CD11b or CD33 with low or absent HLA-DR can identify immature myeloid cells unable to present antigens compatible with MDSCs.[4] [10] [14] Some of these were recently explored in the context of early-stage lung cancers relative to PD-L1 co-expression for predictivity of adjuvant chemotherapy benefit.[15]

Using multiplexed quantitative immunofluorescence (QIF) and simultaneous detection of multiple tumor and myeloid cell markers, we studied the expression, biological context, and clinical significance of major myeloid cell populations in human NSCLC.
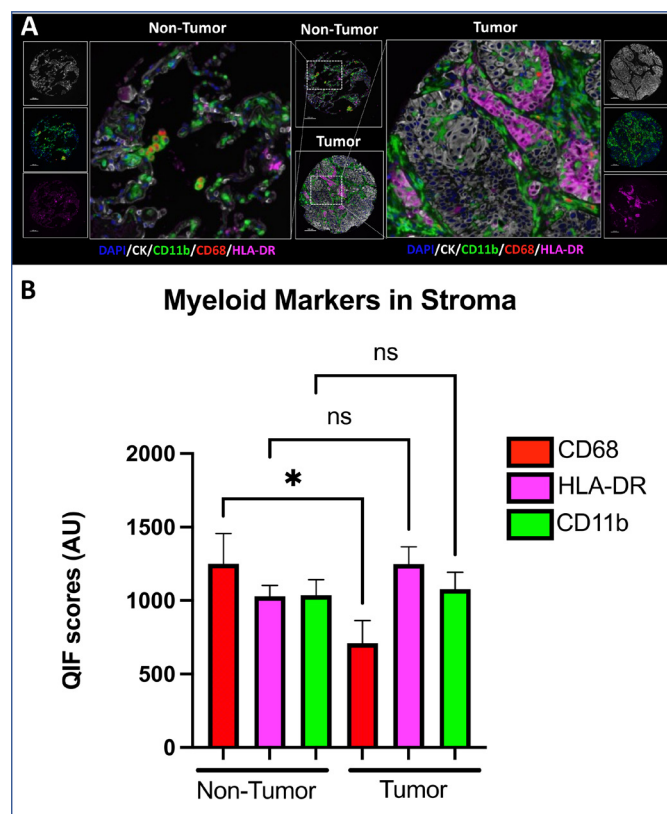

Figure 1 Decreased levels of differentiated myeloid cells in tumor versus non-tumor samples. (A) Representative images of non-tumor (left) and tumor (right) with respect to CD11b, CD68, and HLA-DR expression. (B) Statistically significantly higher QIF level of differentiated myeloid cell marker (CD68) in non-tumor than in tumor cells (p=0.0165). AU, AQUA units; CK, cytokeratin; DAPI, 4',6-Diamidino-2-Phenylindole; QIF, quantitative immunofluorescence.

METHODS
Patient cohorts and tissue microarrays
Formalin-fixed paraffin-embedded (FFPE) samples from three previously reported and well-characterized retrospective collections of NSCLC represented in tissue microarrays (TMA) were included in the study (Cohorts 1–3).[16–19] Cohorts 1 and 2 include independently collected primary lung cancer specimens from Yale University and Greek hospitals, respectively. Cohort 3 includes lung adenocarcinomas from Yale clinically tested for oncogenic mutations in EGFR and KRAS. Finally, we also included a collection of matched-normal tissue and NSCLC from 30 patients who underwent primary resections (Cohort 4). All cases included in this study received standard of care treatment preceding the clinical use of immunotherapy. Thus, no patients in these cohorts were treated with immune checkpoint inhibitors prior to sample acquisition. A detailed description of the four cohorts used in the study is provided in the online supplemental table S1.

TMAs were prepared using standard procedures as described elsewhere,[20] entailing pathology review of H&E-stained preparations followed by 0.6 mm core retrieval from original paraffin blocks via needle into a recipient block. To capture intratumor heterogeneity, at least two cores obtained from different tumor regions
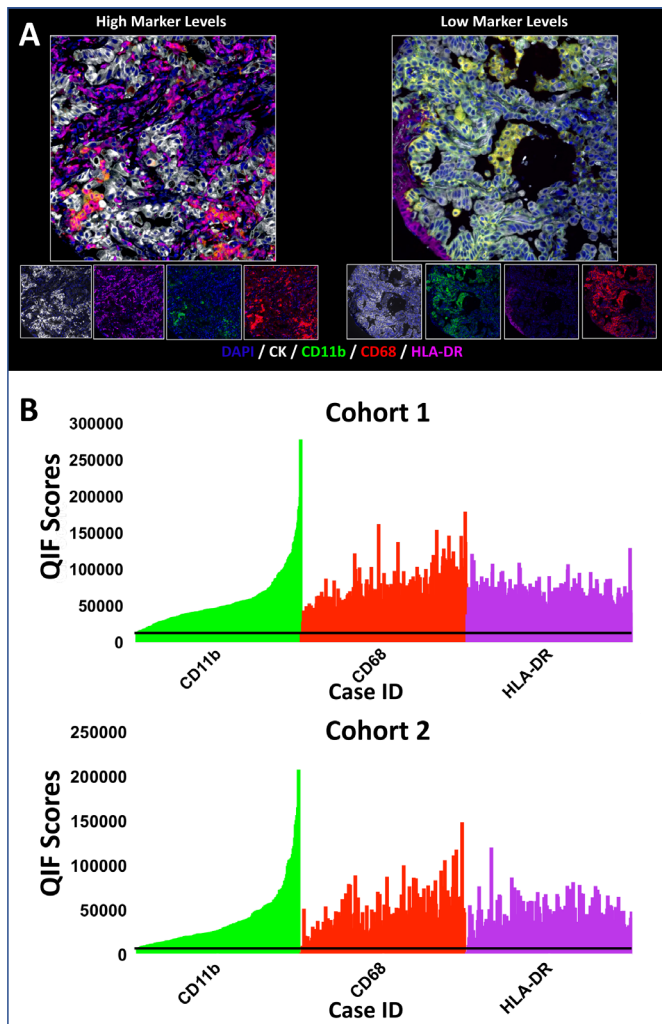
Figure 2 Distribution of marker levels in the main cohorts. (A) Representative images of tumor samples containing high (left) and low (right) levels of CD11b, CD68, and HLA-DR. (B) Distribution of marker levels by case for each marker in each cohort. Cases are ordered from lowest to highest level of CD11b within each cohort. Black lines indicate the visual detection threshold in each cohort. CK, cytokeratin; DAPI, 4',6-Diamidino-2-Phenylindole; QIF, quantitative immunofluorescence.

were included in the TMAs. Because sections from two blocks containing cores from different tumor regions were measured for each cohort and some cases were represented more than once in each block, a minimum of two cores and maximum of four cores were included for each case.

Myeloid cell marker assay validation and reproducibility assessment

We developed a panel of protein markers to distinguish myeloid cell subtypes in the tumor-cell and stromal area of human NSCLC samples. This included 4',6-Diamidino-2-Phenylindole (DAPI) to highlight all cells, pan-cytokeratin (CK) to mark tumor cells, CD11b to identify all myeloid cells, CD68 for mature/differentiated 'M1-like' macrophages, and HLA-DR to indicate

maturation state/antigen-presenting potential. Index TMAs containing non-tumor tissues and positive/negative control FFPE cell line preparations were used to validate the assay specificity and protocol optimization (online supplemental figure S1). The CD11b antibody was tested in TMAs including positive (KG1 and THP-1) and negative (Jurkat) control cell lines on the basis of reported messenger RNA expression levels. Similarly, HLA-DR was tested in positive (221-T1 (+)) and negative (0.174 lymphoblastoma cell line (−)) cell line preparations, and CD68 was tested in KG1a cells with and without short interfering RNA-based CD68 knockdown.

Multiplexed myeloid cell immunofluorescence staining

The five-color multiplexing myeloid-cell QIF protocol was based on the utilization of isotype-specific primary antibodies and horseradish peroxidase (HRP) quenching steps using benzoic hydrazide, as previously reported by our group.[17 21] Briefly, TMA slides were deparaffinized and subjected to antigen retrieval with EDTA buffer (Sigma-Aldrich, St Louis, Missouri, USA) pH=8.0 and boiled for 20 min at 97°C in a pressure-boiling container (PT module, Lab Vision). Endogenous peroxidase activity was dually blocked with peroxidase in methanol for 30 min at room temperature, followed by bovine serum albumin (BSA) with Tween. Overnight incubation at 4°C with primary monoclonal antibody for HLA-DR (mouse IgG2b 1:4000, LS Bio) was followed by 1 hour coincubation of primary CD68 antibody (mouse IgG1 1:1000, Dako) and CD11b (rabbit 1:100, Cell Signaling Technology) at room temperature. HRP-conjugated secondary antibody incubation was sequenced after each primary antibody incubation step (anti-mouse IgG2b; goat anti-rabbit; mouse Envision), and followed by blocking with benzoic hydrazide 0.136 g in 50 µL hydrogen peroxide with 10 mL phosphate-buffered saline. A conjugated cytokeratin antibody (MCK-FITC, 488-AE1/AE3 1:100) was then incubated at room temperature for 1 hour, followed by DAPI at 1:1000 dilution. All steps were separated by washing with BSA.

Fluorescence measurement, scoring, and cutpoint selection

Measurement of the fluorescent signal was performed using the AQUA method of QIF (Navigate Biopharma, Carlsbad, California, USA). This strategy enabled objective and sensitive measurement of targets within user-defined tissue compartments.[16] Briefly, the QIF score of each marker in the CK-positive tumor-cell compartment, the surrounding CK-negative non-tumor/stromal-cell tissue area, or in the CD11b-positive myeloid-cell compartment was calculated by dividing the target pixel intensities by the area of CK-positive or CK-negative pixels. This allows for comparisons across cases with dissimilar tumor and stromal content. Scores were then normalized to the exposure time at which the images were captured in the multispectral analyzer, allowing scores collected at different exposure times to be comparable. The full formula for each normalized pixel value was:

Table 1 Marker AQUA scores by clinicopathologic variable

Marker	Cohort 1 (N=379)				Cohort 2 (N=247)			
	CD11b	CD68	HLA-DR	N	CD11b	CD68	HLA-DR	N
Age								
<65	29,798 p=0.23	3672 p=0.75	17,699 p=0.04	157	17,334 p=0.27	13,224 p=0.92	7215 p=0.70	115
>65	32,793	3720	16,052	211	18,075	1415	8180	132
Gender								
Male	33,100 p=0.04	3720 p=0.84	17,231 p=0.76	173	17,999 p=0.28	1420 p=0.13	8049 p=0.42	196
Female	29,870	3672	17,086	199	16,557	1140	7842	31
Histology								
ADC	32,987 p=0.0001	3840 p=0.008	17,247 p>0.99	202	18,905 p=0.0002	1505 p=0.22	8728 p=0.10	87
SCC	51,473	4766	17,288	86	28,003	1813	10,009	111
Other	36,230	3683	15,053	72	20,767	1253	7764	30
Smoking								
Ever smoker	32,387 p=0.09	3815 p=0.05	16,836 p=0.83	296	17,897 p=0.77	1422 p=0.72	8160 p=0.62	183
Never smoker	28,103	3135	17,228	44	19,449	1390	8485	19
Stage								
I–II	32,527 p=0.74	3797 p=0.59	17,482 p=0.16	279	19,763 p=0.97	1591 p=0.95	10,483 p=0.82	136
III–IV	31,667	3537	17,057	72	22,453	1749	9524	87

ADC, adenocarcinomas; SCC, squamous cell carcinomas.
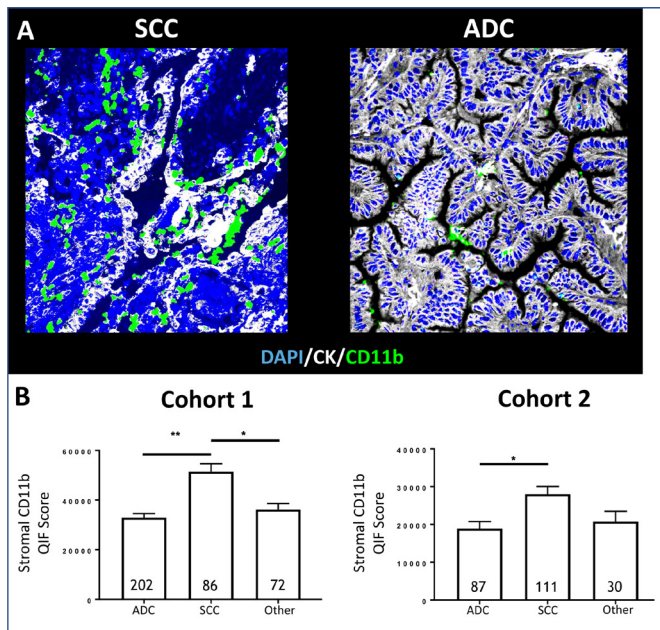
Figure 3 Squamous cell carcinomas contain increased levels of stromal CD11b than adenocarcinomas. (A) Representative images of CD11b levels in the stroma of squamous-cell carcinoma (SCC, left) and adenocarcinoma (ADC, right) specimens. (B) Stromal CD11b was higher in SCC than in ADC in cohort 1 (p=0.0001) and cohort 2 (p=0.0002). Stromal CD11b was statistically significantly higher in SCC than in other tumor histologies in cohort 1 (p=0.0004) but not cohort 2. CK, cytokeratin; DAPI, 4',6-Diamidino-2-Phenylindole; QIF, quantitative immunofluorescence.

$$Normalized\ Pixel\ Value = \frac{Pixel\ Value}{MaxPixel*Exposure\ Time}$$

Finally, all the stained slides were examined by visual inspection and cases or sample areas with staining or tissue artifacts were excluded from the analysis.

Statistical analysis

For the statistical analysis, the median marker scores obtained from all available tumor measurements of each case were used. QIF signals between compartments were analyzed using linear regression and correlation functions and expressed as correlation coefficients. The marker levels in all compartments of interest were examined for differences in their associations with clinicopathologic features and compared across cohorts for validation. Differences between marker scores and patient characteristics were compared using the Student's t-test/one-way analysis of variance for continuous variables and χ^2 test for categorical variables. Overall survival functions were compared using Kaplan-Meier estimates, and statistical significance was determined using the log-rank test. The optimal cutpoints for survival analysis of each target in each compartment of interest were obtained using the X-tile software previously described[20] in Cohort 1 and tested for validation in Cohort 2. All p values were based on two-sided tests, and all values under 0.05 were considered statistically significant. Statistical analyses

were performed using JMP Pro software (V.13.0.0, 2016, SAS Institute, Cary, North Carolina, USA) and GraphPad Prism V.7.0 for Windows (GraphPad Software, San Diego, California, USA).

RESULTS

Staining of morphologically normal human lung tissues with the QIF panel yielded expected patterns of myeloid cell infiltration with discrete cells positive for CD11b, CD68 and HLA-DR located predominantly in the stromal tissue areas and lining alveolar walls (figure 1A). Paired tumor samples showed comparable CD11b+ myeloid cell infiltration, but with prominently lower levels of CD68+ M1-like TAMs than the non-tumor counterpart. HLA-DR showed focal positivity in stromal/immune cells and in CK-expressing malignant cells (figure 1B). In additional analysis of fluorescence colocalization, the lung tumor samples showed a lower fraction of CD11b+HLA-DR- cells than the non-tumor lung tissue (online supplemental figure S2). As expected, the levels of HLA-DR were significantly higher in cases where myeloid cell levels of CD68 were high (above the median) than in cases where myeloid cell CD68 levels were lower than the median (online supplemental figure S3). This finding was consistent in all the cohorts analyzed, supporting the notion that this panel of markers has the capacity to distinguish functionally distinct subsets of myeloid cells (eg, greater antigen presentation capacity in cases with higher CD68 myeloid cell content).

The marker levels were comparable in NSCLC Cohorts 1 and 2. The visual detection threshold was below that of the lowest QIF score for each marker, so every tumor contained at least some cells positive for each of the myeloid markers (figure 2B). CD68 levels showed a positive association with CD11b in both cohorts as expected (R^2=0.30 in Cohort 1 and 0.29 in Cohort 2), as a proportion of CD11b+ cells (M1-like macrophages) co-express CD68. HLA-DR levels were not positively correlated with CD11b (R^2=0.04 in Cohort 1 and 0.06 in Cohort 2) or CD68 (R^2=0.09 in Cohort 1 and 0.29 in Cohort 2), which also supports expected immunobiology given that other cell types, such as activated T cells and tumor cells, can upregulate HLA-DR. The marker levels in the tumor-cell compartment were correlated with the stromal levels, with CD68 having the highest degree of correlation across the cohorts (online supplemental figure S4).

The median marker levels were compared across major clinicopathologic variables of the cases in the cohorts including age, gender, histology, smoking status, and stage. In both cohorts, more patients were >65 years of age, smokers, and had early-stage disease. Cohort 1 featured higher proportions of female patients and adenocarcinomas (ADCs) than Cohort 2. The only statistically significant difference in marker levels across both cohorts was with regard to histology, in that stromal CD11b levels were higher in squamous cell carcinomas
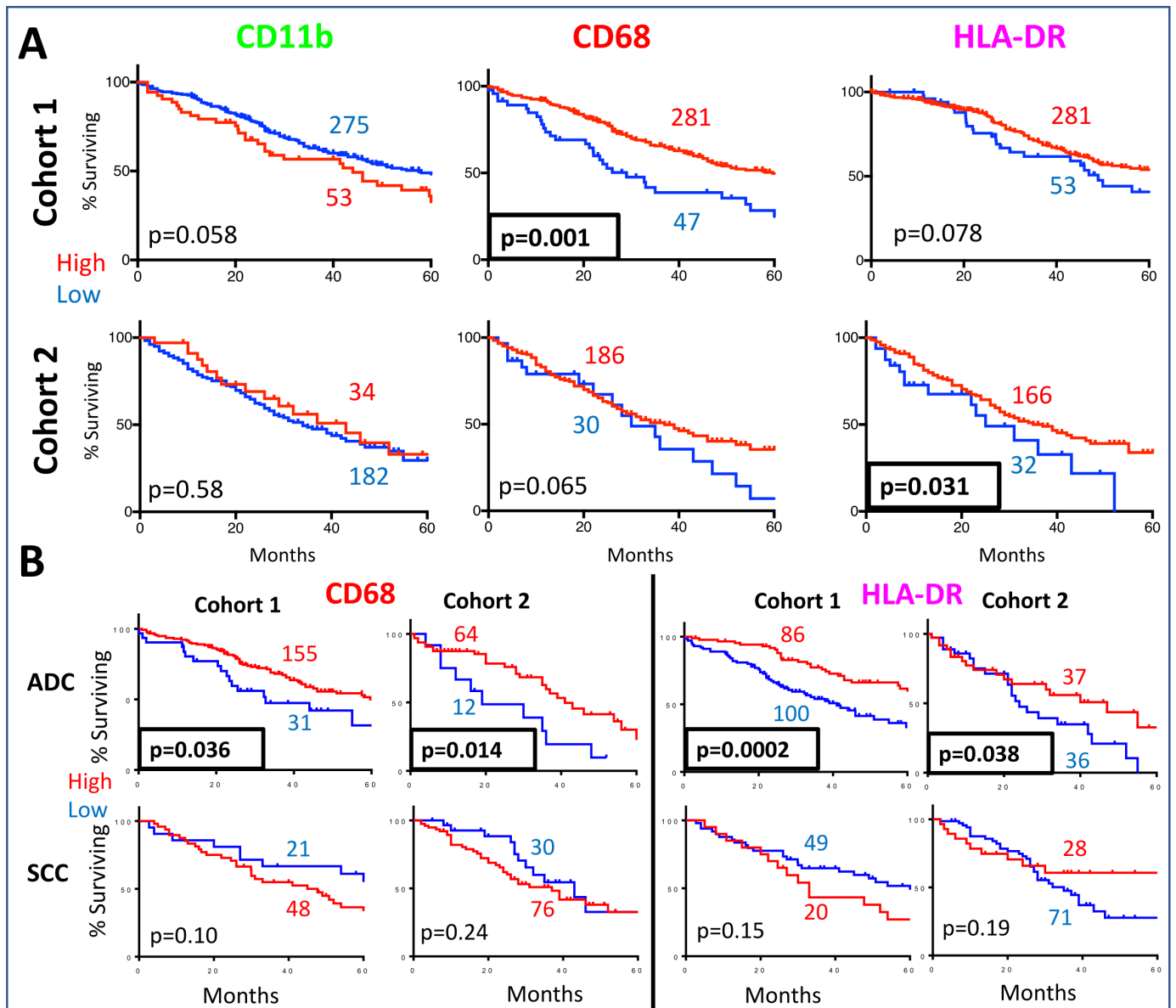
Figure 4 Myeloid markers predict survival in a histology-dependent manner. (A) High (above the median) levels of CD68 associated with survival significantly in Cohort 1 (p=0.001) but not significantly in Cohort 2 (p=0.065). High levels of HLA-DR associated significantly with survival in Cohort 2 (p=0.031), but not in Cohort 1. (B) High levels of CD68 and HLA-DR associated with improved survival in both large cohorts among adenocarcinomas (CD68: p=0.036, p=0.0002; HLA-DR: p=0.014, p=0.038). Among squamous cell carcinomas, high levels of CD68 and HLA-DR did not significantly associate with improved survival, and in fact trended in the opposite direction. ADC, adenocarcinoma; SCC, squamous cell carcinoma.

(SCCs) than in ADCs, and trended towards being higher than in other histotypes (table 1, figure 3).

When measuring the markers in stromal cells, higher levels of CD68 and HLA-DR were associated with longer 5-year overall survival. This effect was statistically significant in Cohort 1 for CD68 (p=0.001) and in Cohort 2 for HLA-DR (p=0.031) using the same marker stratification cutpoints (see **Methods**). These associations were not significant, but had p values close to 0.05 in the independent validation cohorts (p=0.078 and 0.065, respectively). Stromal CD11b levels did not consistently associate with survival across both cohorts (figure 4A). However, in the independent validation cohorts where these markers were not significant, selectively measuring CD68 and HLA-DR

in the CD11b-expressing myeloid cells revealed significant associations between higher CD68 and HLA-DR and longer 5-year survival (online supplemental figure S5).

Because stromal CD11b levels had been found to differ significantly across histologies, we wondered if histologic differences might highlight the myeloid markers' prognostic capacity in NSCLC. In ADCs, higher levels of CD68 (p=0.036 and 0.014, respectively) and HLA-DR (p=0.0002 and 0.038, respectively) statistically predicted for improved 5-year survival across both cohorts using the same stratification cutpoint. In SCCs, these associations were not statistically significant and in fact trended in the opposite direction (figure 4B).
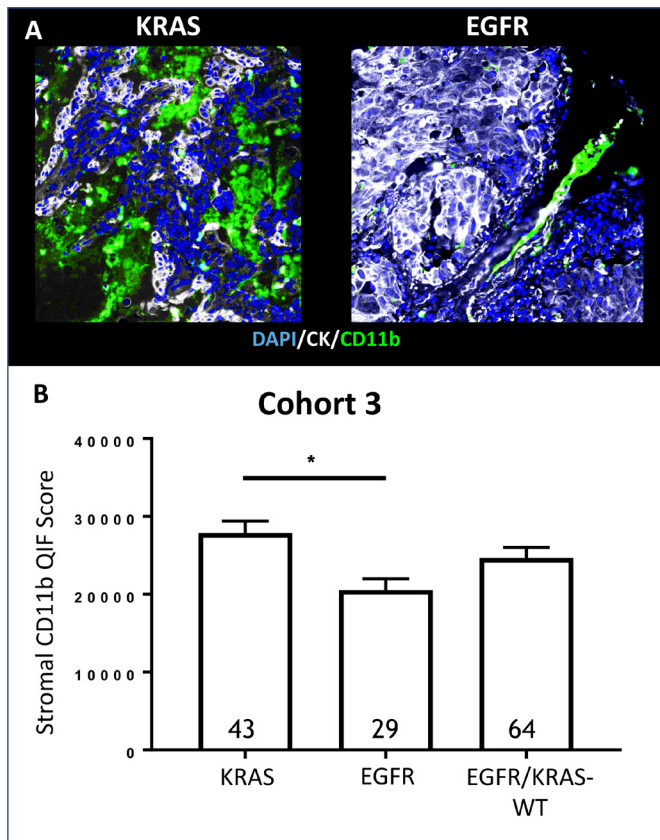
Figure 5 Stromal CD11b levels were significantly higher in KRAS-mutant tumors than in EGFR-mutant tumors. In Cohort 3, the only cohort with annotated KRAS/EGFR mutation status, stromal CD11b levels were higher in KRAS-mutant tumors than in EGFR-mutant tumors (p=0.006). CK, cytokeratin; DAPI, 4',6-Diamidino-2-Phenylindole; QIF, quantitative immunofluorescence; WT, wild type.

To address the association of the myeloid markers with the presence of specific oncogenic driver mutations in lung ADC, we studied a third cohort with molecular annotation (see methods). Analysis of Cohort 3, which included tumors harboring driver mutations in EGFR, KRAS and lung ADCs lacking mutations in both oncogenes, revealed that EGFR-mutated tumors featured lower CD11b+ stromal myeloid-cell content than KRAS-mutant tumors, and trended towards lower levels than EGFR/KRAS-wild-type tumors (figure 5A and B).

DISCUSSION

It is well established that histologic and genetic differences delineate distinct clinical features and treatment paradigms for NSCLC. However, the biological underpinnings of why patients with SCC have not, for example, benefitted from pemetrexed-containing regimens remain elusive. Studies using flow cytometry have revealed differences between ADCs and SCCs with respect to T-cell subtypes, macrophage, and neutrophil content[22]; however, the impact of these findings on survival has not been examined. Our study provides evidence for distinct histology-dependent myeloid cell compositions that appear to have differential, context-specific prognostic capacity.

Our results indicate that lung ADCs have lower myeloid cell infiltration than SCCs and that increased levels of CD68+ and HLA-DR+ cells in the stromal area are associated with better outcome only in the former histology variant. This result is consistent with previous studies,[23–26] and suggests that accumulation of classically polarized or M1-like cells has a favorable immunomodulatory role in these malignancies. The dissimilar levels of myeloid cell infiltration across lung ADCs with oncogenic KRAS and EGFR mutations indicate a different myeloid immune contexture of these malignancies that could be exploited therapeutically. Our results agree with previous studies indicating different local adaptive immune responses such as PD-L1 expression and CD8+ T cell infiltration across ADCs with different oncogenic drivers.[27]

Our findings using direct protein-based spatial mapping and visualization of the myeloid markers in tumor specimens suggest that SCCs may have higher content of less favorable myeloid cells. While not statistically significant and with power limitations due to the low frequency of SCC in the cohorts (as expected for western populations), the trend towards worse outcomes seen with higher CD68 and HLA-DR levels in SCCs warrants further exploration. For example, a recent single-cell analysis of myeloid cells in a cohort of esophageal SCCs, which are histologically and genomically similar to lung SCCs,[28 29] revealed correlation between M1-like and M2-like phenotypes, nominating an immunosuppressive phenotype even for CD68+ myeloid cells in this context.[30] Indeed, CD38+ MDSCs have been shown to correlate with adverse outcomes in esophageal SCC that is abrogated with their inhibition.[31]

A limitation of our study is that the large cohorts analyzed included primarily specimens from patients treated prior to regular molecular testing and the advent of immunotherapy, so it is unclear if the survival effect of the unveiled immunobiology in this study will translate to cases treated with immunotherapy regimens. Methodologically, TMAs include only relatively small (0.6 mm) tumor areas, making it possible to over-represent or under-represent the markers due to possible intra-tumor heterogeneity. We strove to overcome this at least in part by including TMA cores from at least two separate tumor areas, as well as the robustness afforded by confirmation of clinicopathologic findings from one cohort in an independent cohort. Interestingly, the analysis of the intratumor heterogeneity of the myeloid markers by comparing measurements in cores from different tumor areas indicates a modest but significant positive correlation (online supplemental figure S6). While this indicates some degree of concordance of the markers across different tumor areas, it emphasizes the need to perform multiple measurements to achieve reliable results. Future studies using full-face whole tissue specimens and including multiple tumor areas will be required to adequately characterize the impact of spatial

heterogeneity on myeloid cell subpopulations and prognosis.

Compared with other studies of myeloid cells in lung cancer, our study's strengths lie in the rigorous validation procedures employed for both the individual components and multiplexed myeloid cell panel. Application of this novel assay to two large, clinically annotated, independent cohorts provides a degree of generalizability to our results. To confirm the true clinical significance of these findings, carefully designed prospective studies of treated patients aimed to delineate myeloid cell populations across histologic and molecular subtypes will be required. In particular, the suggestion of distinct myeloid cell contexture and clinical significance in SCC may deserve dedicated biomarker and therapeutic development.

Data availability statement Data are available upon reasonable request. Additional data is provided as supplementary information.

Supplemental material This content has been supplied by the author(s). It has not been vetted by BMJ Publishing Group Limited (BMJ) and may not have been peer-reviewed. Any opinions or recommendations discussed are solely those of the author(s) and are not endorsed by BMJ. BMJ disclaims all liability and responsibility arising from any reliance placed on the content. Where the content includes any translated material, BMJ does not warrant the accuracy and reliability of the translations (including but not limited to local regulations, clinical guidelines, terminology, drug names and drug dosages), and is not responsible for any error and/or omissions arising from translation and adaptation or otherwise.

ORCID iDs
Brian S Henick http://orcid.org/0000-0003-2681-0805
Franz Villarroel-Espindola http://orcid.org/0000-0003-0080-2444
Jovian Yu http://orcid.org/0000-0001-9214-7576
Shruti Desai http://orcid.org/0000-0002-5234-5890
David L Rimm http://orcid.org/0000-0001-5820-4397
Kurt A Schalper http://orcid.org/0000-0001-5692-4833

REFERENCES

1 De Kleer I, Willems F, Lambrecht B, *et al*. Ontogeny of myeloid cells. *Front Immunol* 2014;5:423.
2 Okabe Y, Medzhitov R. Tissue-specific signals control reversible program of localization and functional polarization of macrophages. *Cell* 2014;157:832–44.
3 Davies LC, Taylor PR. Tissue-resident macrophages: then and now. *Immunology* 2015;144:541–8.
4 Gabrilovich DI. Myeloid-derived suppressor cells. *Cancer Immunol Res* 2017;5:3–8.
5 Liu Y, Zugazagoitia J, Ahmed FS, *et al*. Immune cell PD-L1 colocalizes with macrophages and is associated with outcome in PD-1 pathway blockade therapy. *Clin Cancer Res* 2020;26:970–7.
6 Holt PG, Strickland DH, Wikström ME, *et al*. Regulation of immunological homeostasis in the respiratory tract. *Nat Rev Immunol* 2008;8:142–52.
7 Franklin RA, Li MO. Ontogeny of tumor-associated macrophages and its implication in cancer regulation. *Trends Cancer* 2016;2:20–34.
8 Qian B-Z, Pollard JW. Macrophage diversity enhances tumor progression and metastasis. *Cell* 2010;141:39–51.
9 Zhang Q-wen, Liu L, Gong C-yang, *et al*. Prognostic significance of tumor-associated macrophages in solid tumor: a meta-analysis of the literature. *PLoS One* 2012;7:e50946.
10 Mantovani A, Marchesi F, Malesci A, *et al*. Tumour-associated macrophages as treatment targets in oncology. *Nat Rev Clin Oncol* 2017;14:399–416.
11 Ma J, Liu L, Che G, *et al*. The M1 form of tumor-associated macrophages in non-small cell lung cancer is positively associated with survival time. *BMC Cancer* 2010;10:112.
12 Mei J, Xiao Z, Guo C, *et al*. Prognostic impact of tumor-associated macrophage infiltration in non-small cell lung cancer: a systemic review and meta-analysis. *Oncotarget* 2016;7:34217–28.
13 Murray PJ, Allen JE, Biswas SK, *et al*. Macrophage activation and polarization: nomenclature and experimental guidelines. *Immunity* 2014;41:14–20.
14 Bronte V, Brandau S, Chen S-H, *et al*. Recommendations for myeloid-derived suppressor cell nomenclature and characterization standards. *Nat Commun* 2016;7:12150.
15 Gross DJ, Chintala NK, Vaghjiani RG, *et al*. Tumor and tumor-associated macrophage programmed Death-Ligand 1 expression is associated with adjuvant chemotherapy benefit in lung adenocarcinoma. *J Thorac Oncol* 2022;17:89–102.
16 Velcheti V, Schalper KA, Carvajal DE, *et al*. Programmed death ligand-1 expression in non-small cell lung cancer. *Lab Invest* 2014;94:107–16.
17 Schalper KA, Brown J, Carvajal-Hausdorf D, *et al*. Objective measurement and clinical significance of TILs in non-small cell lung cancer. *J Natl Cancer Inst* 2015;107. doi:10.1093/jnci/dju435. [Epub ahead of print: 03 02 2015].

18 Anagnostou VK, Syrigos KN, Bepler G, *et al*. Thyroid transcription factor 1 is an independent prognostic factor for patients with stage I lung adenocarcinoma. *J Clin Oncol* 2009;27:271–8.

19 Toki MI, Carvajal-Hausdorf DE, Altan M, *et al*. EGFR-GRB2 protein colocalization is a prognostic factor unrelated to overall EGFR expression or EGFR mutation in lung adenocarcinoma. *J Thorac Oncol* 2016;11:1901–11.

20 Camp RL, Chung GG, Rimm DL. Automated subcellular localization and quantification of protein expression in tissue microarrays. *Nat Med* 2002;8:1323–8.

21 Brown JR, Wimberly H, Lannin DR, *et al*. Multiplexed quantitative analysis of CD3, CD8, and CD20 predicts response to neoadjuvant chemotherapy in breast cancer. *Clin Cancer Res* 2014;20:5995–6005.

22 Kargl J, Busch SE, Yang GHY, *et al*. Neutrophils dominate the immune cell composition in non-small cell lung cancer. *Nat Commun* 2017;8:14381.

23 Rakaee M, Busund L-TR, Jamaly S, *et al*. Prognostic value of macrophage phenotypes in resectable non-small cell lung cancer assessed by multiplex immunohistochemistry. *Neoplasia* 2019;21:282–93.

24 Zhang B, Yao G, Zhang Y, *et al*. M2-polarized tumor-associated macrophages are associated with poor prognoses resulting from accelerated lymphangiogenesis in lung adenocarcinoma. *Clinics* 2011;66:1879–86.

25 Dai F, Liu L, Che G, *et al*. The number and microlocalization of tumor-associated immune cells are associated with patient's survival time in non-small cell lung cancer. *BMC Cancer* 2010;10:220.

26 Welsh TJ, Green RH, Richardson D, *et al*. Macrophage and mast-cell invasion of tumor cell islets confers a marked survival advantage in non-small-cell lung cancer. *J Clin Oncol* 2005;23:8959–67.

27 Toki MI, Mani N, Smithy JW, *et al*. Immune marker profiling and programmed death ligand 1 expression across NSCLC mutations. *J Thorac Oncol* 2018;13:1884–96.

28 Lin EW, Karakasheva TA, Lee D-J, *et al*. Comparative transcriptomes of adenocarcinomas and squamous cell carcinomas reveal molecular similarities that span classical anatomic boundaries. *PLoS Genet* 2017;13:e1006938.

29 Dotto GP, Rustgi AK. Squamous cell cancers: a unified perspective on biology and genetics. *Cancer Cell* 2016;29:622–37.

30 Zheng Y, Chen Z, Han Y, *et al*. Immune suppressive landscape in the human esophageal squamous cell carcinoma microenvironment. *Nat Commun* 2020;11:6268.

31 Karakasheva TA, Waldron TJ, Eruslanov E, *et al*. CD38-Expressing myeloid-derived suppressor cells promote tumor growth in a murine model of esophageal cancer. *Cancer Res* 2015;75:4074–85.